Original Article

Integrated analysis of long non-coding RNAs and mRNAs associated with peritendinous fibrosis

Wei Zheng [a,1], Chen Chen [a,b,1], Shuai Chen [a], Cunyi Fan [a,*], Hongjiang Ruan [a,*]

[a] Department of Orthopaedics, Shanghai Jiao Tong University Affiliated Sixth People's Hospital, 600 Yishan Road, Shanghai 200233, China
[b] Department of Arthroscopic Surgery, Shanghai Sixth People's Hospital, Shanghai Jiao Tong University, Shanghai, China

HIGHLIGHTS

- RNA-seq identified 20646 lncRNAs in peritendinous tissues.
- A total of 219 lncRNAs and 3403 mRNAs were differentially expressed during fibrosis progression.
- Bioinformatics analysis revealed enriched functions of dysregulated mRNAs.
- Possible lncRNA-mRNA interactions were examined using a co-expression network.
- Silencing of dnm3os prevented profibrotic changes in primary tenocytes.

GRAPHICAL ABSTRACT
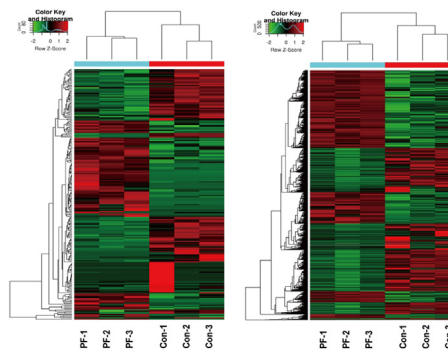
ARTICLE INFO

ABSTRACT

The dysregulation of long non-coding RNAs (lncRNAs) is associated with the development of various diseases. However, little is known about the regulatory function of lncRNAs in peritendinous fibrosis. Therefore, the expression profiles of lncRNAs and mRNAs in normal tendon and fibrotic peritendinous tissues were analyzed in this study using RNA sequencing. In total, 219 lncRNAs and 3403 mRNAs were identified that were differentially expressed between the two sets of tissues. Gene Ontology and Kyoto Encyclopedia of Genes and Genomes pathway analyses revealed that the dysregulated mRNAs were mainly associated with immune regulation, inflammation, extracellular matrix (ECM) production and remodeling, and cell cycle regulation. An lncRNA-mRNA co-expression network revealed 181 network pairs comprising eight dysregulated lncRNAs and 146 mRNAs. The results of the bioinformatics analysis indicated that the dysregulated lncRNAs play a role in fibrogenesis through regulation of the cell cycle, inflammation, and ECM production. Furthermore, silencing the lncRNA dnm3os prevented transforming growth factor (TGF)-β1-induced tenocyte proliferation and expression of genes related to fibrogenesis. These findings provide a basis for investigations into the regulatory mechanisms underlying the development and progression of peritendinous fibrosis.

Introduction

Peritendinous fibrosis is a common complication after tendon injury and is characterized by excessive extracellular matrix (ECM) accumulation due to disruption of the balance between ECM synthesis and degradation [1,2]. This imbalance results in impaired tendon function and an increased risk of recurrence after

surgical intervention. Fibroblasts undergo myofibroblastic transdifferentiation, which is regulated by a number of cytokines and growth factors including transforming growth factor (TGF), which is critical for fibrogenesis [3,4]. Although previous studies have examined the molecular basis of peritendinous fibrosis, the factors that trigger this process have not been clearly elucidated.

Only a small percentage of the mammalian genome encodes proteins; most RNAs are non-coding and have a regulatory function. LncRNAs, which are longer than 200 bp, have been widely investigated in various physiological and pathological contexts by high-throughput RNA sequencing (RNA-seq) and bioinformatics analysis; however, their role in peritendinous fibrosis is not clear [5–7].

To address this issue, in the present study, RNA-seq was performed to obtain the lncRNA and mRNA expression profiles of normal tendon and fibrotic peritendinous tissues; Gene Ontology (GO) and Kyoto Encyclopedia of Genes and Genomes (KEGG) pathway enrichment analyses were then carried out to identify transcripts that were differentially expressed between the two sets of samples. Additionally, possible lncRNA-mRNA interactions associated with fibrogenesis and the mechanisms underlying the development of peritendinous fibrosis were examined.

Material and methods

Tendon tissue samples

Tendon tissue samples and personal data were obtained from patients who had undergone surgery at our hospital. In the peritendinous fibrosis group, early-stage fibrotic peritendinous tissue samples were obtained from patients who underwent tendon repair surgery 2–3 weeks after initial tendon injury. All patients exhibited peritendinous adhesion. In the control group, tendon tissue samples were harvested from patients undergoing forearm amputation in the emergency operating room. All tendon tissues were harvested intraoperatively and were immediately stored in liquid nitrogen until use. Peritendinous fibrosis and paired normal tendon samples (n = 3 each) were used for global lncRNA and mRNA profiling and for the confirmation of peritendinous fibrosis based on collagen (COL)1 and α-smooth muscle actin (α-SMA) expression levels. *Experiments were approved by the Ethics Committee of the Shanghai Sixth People's Hospital East Campus (approval no. 2017–021), and written-informed consent was obtained from all participants.*

Cell culture and treatments

Primary tenocytes were isolated from mouse Achilles tendon tissues. Briefly, tendon tissues were cut into 1 mm^3 pieces and digested with 0.15% collagenase NB4 (SERVA, Germany) for 2 h. Subsequently, the suspension was filtered through cell meshes and centrifuged at 1000 rpm for 5 min. Cell pellets were resuspended in the culture medium (Dulbecco's modified Eagle medium supplemented with 10% fetal bovine serum and 1% penicillin-streptomycin) at 37 °C with 5% CO_2. Tenocytes were treated with 2 ng/ml TGF-β1 (R&D systems, Minneapolis, MN, United States). Then, siRNA transfection was performed using Lipofectamine 2000, according to the manufacturer's procedures.

RNA isolation, library construction, and sequencing analysis

Total RNA was extracted from tendon tissues using TRIzol reagent (Invitrogen, Carlsbad, CA, USA) according to the manufacturer's instructions. rRNAs were removed from total RNA using the Ribo-Zero rRNA Removal kit (Illumina, San Diego, CA, USA) according to the manufacturer's instructions. RNA purity was evaluated with a NanoDrop ND-2000 spectrophotometer (Thermo Fisher Scientific, Waltham, MA, USA), and RNA integrity was assessed by denaturing agarose gel electrophoresis. RNA libraries were constructed using rRNA-depleted RNAs with the TruSeq Stranded Total RNA Library Prep kit (Illumina, San Diego, CA, USA) according to the manufacturer's instructions. Library quality was assessed and quantitation was performed with a BioAnalyzer 2100 (Agilent Technologies, Santa Clara, CA, USA); 10 pM RNA libraries were denatured as single-stranded DNA molecules, captured on Illumina flow cells, amplified *in situ* as clusters, and sequenced for 150 cycles on an Illumina HiSeq 4000 sequencer.

High-throughput lncRNA sequencing and bioinformatics analyses were performed by Cloud-Seq Biotech (Shanghai, China). Briefly, paired-end reads were harvested from the sequencer, and quality controlled was performed based on Q30. After 3′ adaptor trimming and the removal of low-quality reads with Cutadapt software (v1.9.3), high-quality trimmed reads were aligned to the human reference genome (University of California at Santa Cruz hg19). Using the Ensembl gtf gene annotation file with hisat2 software (v2.0.4), Cuffdiff software (v2.2.1, part of cufflinks) was used to obtain gene level fragments per kilobase of exon per million (FPKM) reads as lncRNA and mRNA expression profiles; fold change and *P* values were calculated based on the FPKM data. LncRNAs and mRNAs with a fold change ≥1.5 and *P* < 0.05 were deemed as differentially expressed.

GO and KEGG pathway analyses

GO and KEGG pathway enrichment analyses were performed based on the information on differentially expressed mRNAs [6,8]. GO analysis provides a controlled vocabulary for describing gene and gene product attributes in any organism (http://www.geneontology.org). GO covers three domains: biological process, cellular component, and molecular function. The Fisher's exact test was used to determine whether the overlap between the gene and GO annotation lists was larger than expected by chance. The KEGG database was used for pathway analysis. *P* < 0.05 was considered to indicate the significant enrichment of differentially expressed genes.

Quantitative real-time polymerase chain reaction (qRT-PCR) verification

One microgram of total RNA was converted into cDNA using the PrimeScript RT Reagent kit (Takara Bio, Otsu, Japan) according to the manufacturer's instructions. qRT-PCR was performed using the SYBR Green Real-time PCR kit (Takara Bio). Primer sequences were designed using Primer 5.0 software (Premier Biosoft, Palo Alto, CA, USA). The lncRNA and mRNA expression data were normalized to the β-actin expression level. Relative gene expression levels were calculated with the $2^{-\Delta\Delta Ct}$ method. The experiment was repeated three times.

LncRNA-mRNA Co-expression network analysis

Co-expression networks were constructed to evaluate correlations among the expressed genes. To determine the relationships between dysregulated lncRNAs and mRNAs, the Pearson's correlation coefficient (PCC) between coding and non-coding genes was calculated, and those with PCC ≥ 0.990 were selected. The co-expression network of lncRNA-mRNA interactions was visualized using Cytoscape software (http://www.cytoscape.org/).

Cell viability analysis

Cell viability was assessed by cell counting kit (CCK)8 (Dojindo, Japan). Tenocytes were cultured at a density of 3×10^3 cells per well and treated for 48 h. Cell viability was assessed by incubating each well with 100 μL of CCK8 solution for 2 h at 37 °C and measuring the absorbance at 450 nm.
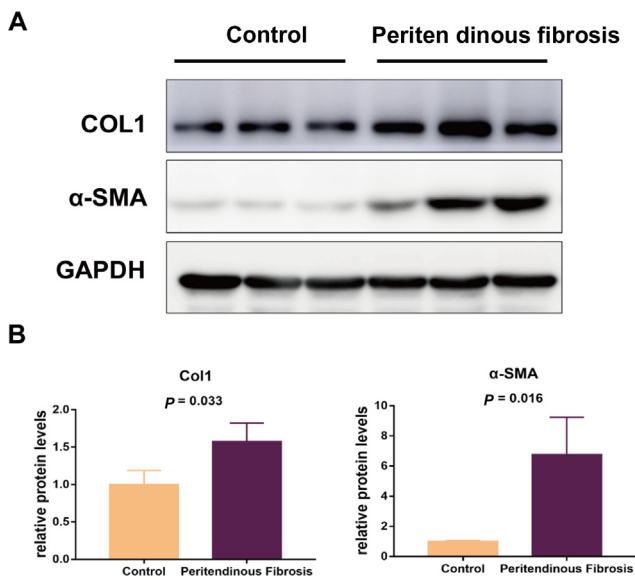
Statistical analysis

Data were analyzed using SPSS 21.0 software (SPSS Inc., Chicago, IL, USA). Differences between groups were evaluated with a two-tailed Student's t-test. Statistical analyses were performed with a significance level of $\alpha = 0.05$ ($P < 0.05$).

Results

Identification of LncRNAs in human tendon tissues

Before RNA-seq, COL1 and α-SMA expression levels were evaluated to confirm the occurrence of fibrogenesis in early-stage adhesive tissues. Western blot analysis showed that COL1 and α-SMA protein expression was higher in early-stage fibrotic peritendinous tissues than in normal control tendon tissues (Fig. 1A, B).
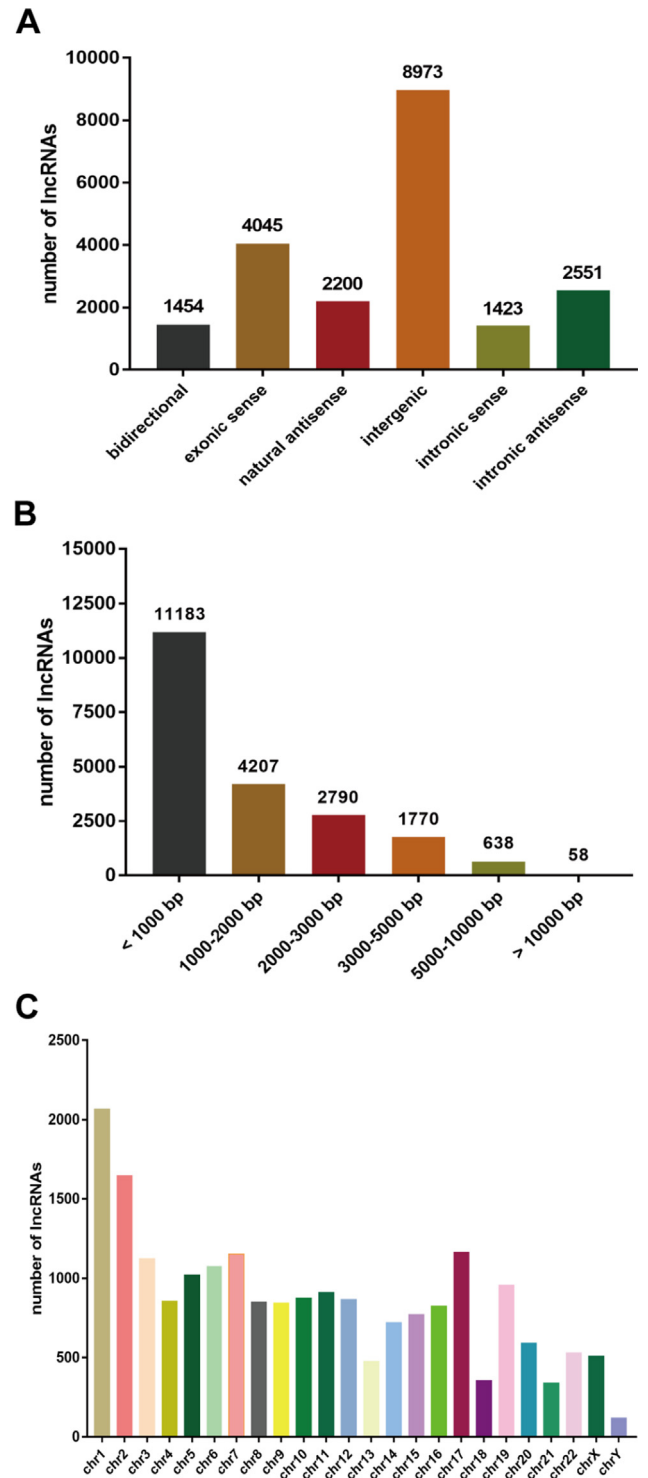
Transcriptomic analyses were carried out to assess differences in RNA expression between the peritendinous fibrosis and control groups. The OD260/280 ratio revealed that each sample was of satisfactory quality. RNA-seq of six cDNA libraries yielded over 50 million raw reads with most being clean reads (Table 1). Over

Fig. 2. Features of lncRNAs detected by RNA-seq. (A) Classification of lncRNAs according to localization. (B) Length distribution of lncRNAs. (C) Chromosome distribution of lncRNAs identified in tendon tissues.

Fig. 1. Evaluation of fibrogenesis in tendon and fibrotic peritendinous tissues. (A) COL1 and α-SMA protein expression was evaluated by western blotting. (B) Quantification of COL1 and α-SMA protein levels. GAPDH was used for normalization. The tissue samples were from three healthy and three diseased individuals.

Table 1
Summary of draft reads of six libraries by RNA-sequencing.

Sample	Raw reads	Clean reads	Aligned reads	Alignment rates
con-1	69,740,266	69,574,128	58,037,659	83.42%
con-2	66,559,716	66,440,202	54,643,979	82.25%
con-3	71,711,878	71,324,256	56,905,045	79.78%
PF-1	69,106,124	68,325,724	60,157,325	88.04%
PF-2	76,096,036	75,971,682	71,638,736	94.30%
PF-3	67,799,100	67,647,956	56,563,278	83.61%

79.78% of clean reads mapped perfectly to the reference human genome. The RNA-seq identified 20,646 lncRNAs, including 8973 (43%) intergenic, 4045 (20%) exon sense-overlapping, 1454 (7%) bidirectional, 2200 (11%) natural antisense, 1423 (7%) intron sense-overlapping, and 2551 (12%) intronic antisense lncRNAs (Fig. 2A). The average lncRNA length was 1526 bp with 75.4% being shorter than 2000 bp (Fig. 2B). All lncRNAs were widely distributed among human chromosomes 1–22, X, and Y, with chromosome 1 accounting for the largest number of lncRNAs (2066, 10%) (Fig. 2C). The sequencing data have been uploaded to the NCBI Gene Expression Omnibus database (accession no. GSE108933).

Differentially expressed LncRNAs and mRNAs during peritendinous fibrosis progression

To identify lncRNAs involved in the development of peritendinous fibrosis, RNA-seq was performed to reveal lncRNAs differentially expressed between three pairs of normal tendon and fibrotic peritendinous tissue samples. A total of 219 differentially expressed lncRNAs were identified, including 98 that were upregulated and 121 that were downregulated in fibrotic peritendinous tissues. Among the dysregulated lncRNAs, 18 were bidirectional, 27 were exon sense-overlapping, 164 were intergenic, one was intron sense-overlapping, four were intronic antisense, and five were natural antisense. Of these, 30 and 40 lncRNAs were exclusively expressed in normal tendon and fibrotic peritendinous tissues, respectively. ENST00000362807 was the most highly upregulated (fold change = 56), and ENST00000429829 was the most downregulated (fold change = 102) lncRNA in the peritendinous fibrosis group relative to the level in the control group. In addition, mRNA expression profiles were obtained by RNA-seq. Comparisons of mRNA levels between the two groups revealed 3403 differentially expressed mRNAs, of which 1704 and 1699 were up- and downregulated, respectively, in the fibrotic

peritendinous tissues. Several markers of fibrogenesis including COL1A1, COL3A1, COL5A1, and ACTA2, were upregulated in the fibrotic peritendinous compared to the control tissues. Hierarchical clustering and a heatmap of lncRNAs and mRNAs showed that the three fibrotic peritendinous tissue samples clustered separately from the normal tendon tissue samples (Fig. 3A, B). These results suggest that the lncRNA and mRNA expression levels in fibrotic peritendinous tissues differ from those in matched normal tendon tissues.

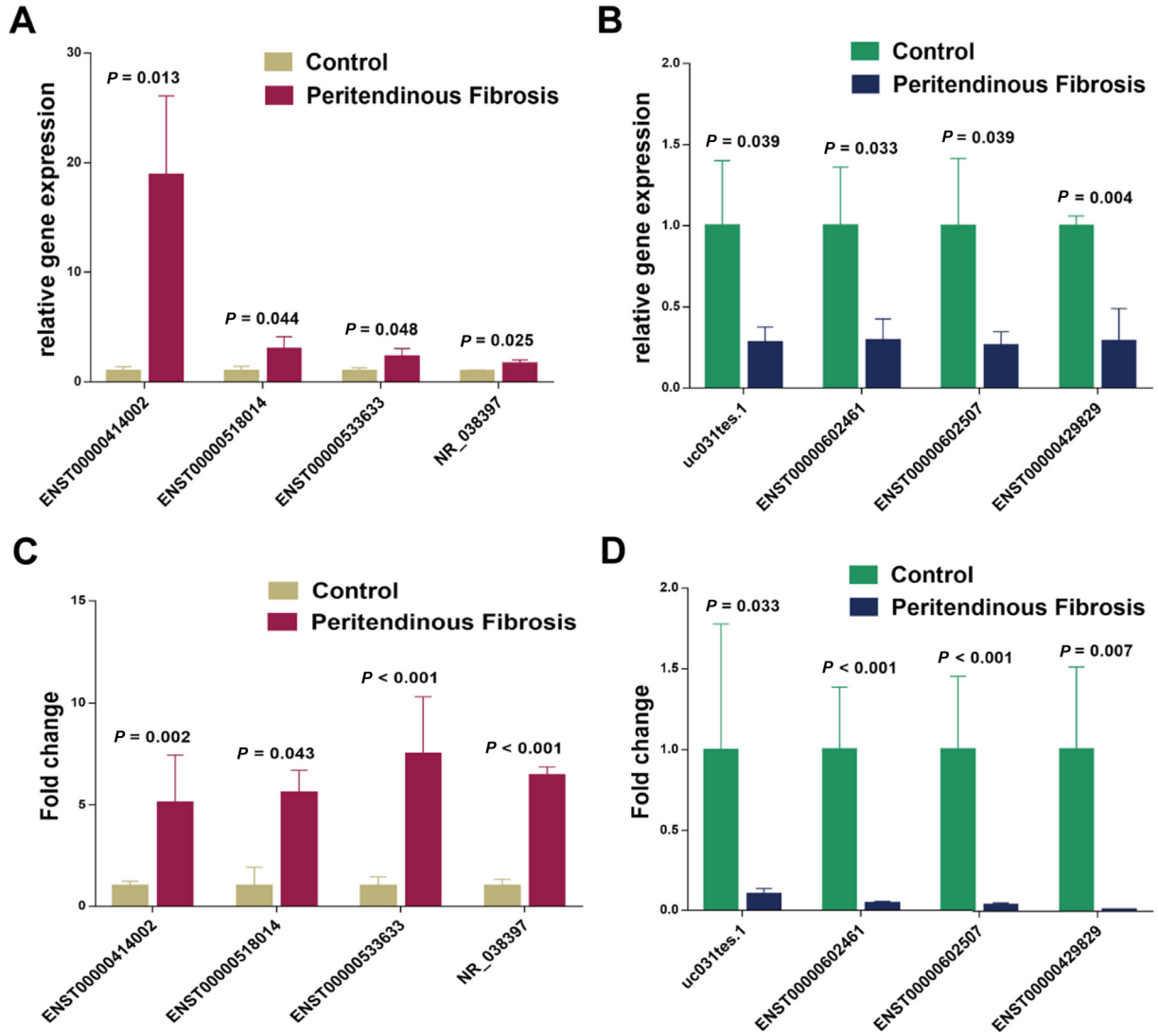### Validation of gene expression profiles using qRT-PCR

The accuracy and reproducibility of the differentially expressed lncRNAs and mRNAs identified by RNA-seq were validated by qRT-PCR. Five and eight differentially expressed mRNAs and lncRNAs were selected for verification, respectively. qRT-PCR data confirmed the RNA-seq results, although the fold change values differed slightly (Figs. 4 and 5). These differentially expressed lncRNAs may be involved in the progression of peritendinous fibrosis.

GO and KEGG pathway analyses

GO enrichment analysis was performed to examine the functions of the differentially expressed mRNAs identified by RNA-seq. GO analysis revealed that the upregulated mRNAs were mostly enriched in biological processes related to cellular component disassembly, translational termination, signal recognition particle (SRP)-dependent cotranslational protein targeting the membrane, cotranslational protein targeting the membrane, and protein targeting the endoplasmic reticulum (ER) (Fig. 6A). On the other hand, the downregulated mRNAs were enriched in cellular responses to chemical stimulus, responses to organic substance, responses to stimulus, multicellular organismal development, single-organism
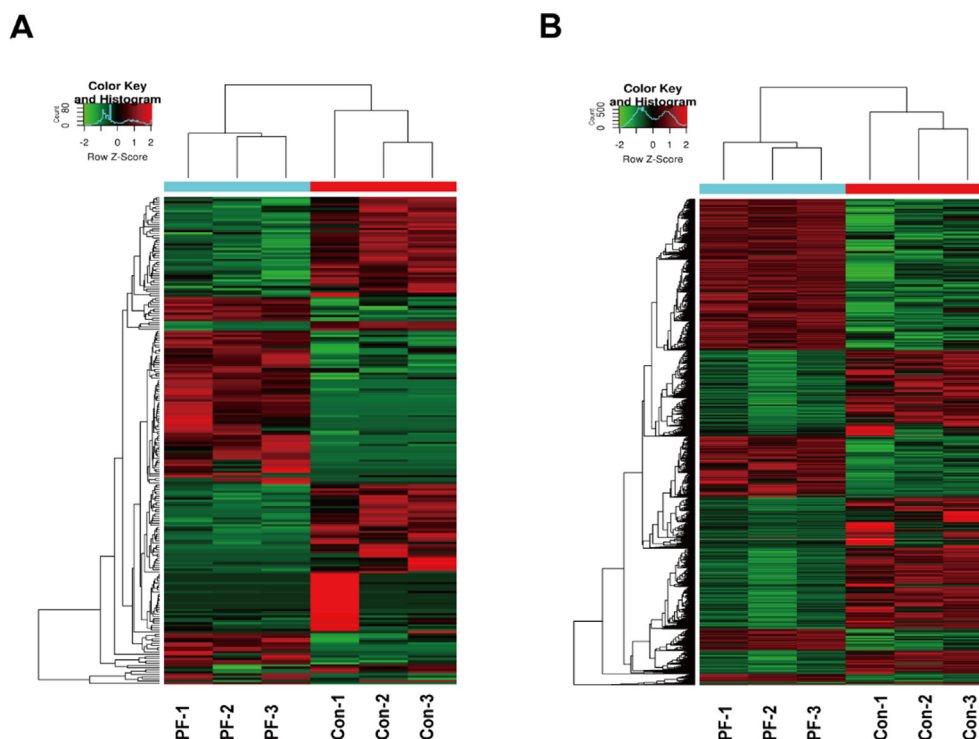
Fig. 3. **Heat map of differentially expressed lncRNAs and mRNAs in fibrotic peritendinous tissues compared to normal tendon tissues.** Each row represents one tissue sample, and each column represents one lncRNA (A) or mRNA (B). Relative lncRNA or mRNA expression is depicted according to the color scale. Red color indicates upregulation; green indicates downregulation; −2, 0, 1, and 2 represent fold changes in the corresponding spectrum.

Fig. 4. qRT-PCR validation of differentially expressed lncRNAs. (A) qRT-PCR verification of the expression profiles of 4 upregulated lncRNAs in fibrotic peritendinous tissues. (B) qRT-PCR verification of the expression profiles of 4 downregulated lncRNAs in fibrotic peritendinous tissues. (C) Fold changes of 4 upregulated lncRNAs in fibrotic peritendinous tissues identified by RNA-seq. (D) Fold changes of 4 downregulated lncRNAs in fibrotic peritendinous tissues identified by RNA-seq.
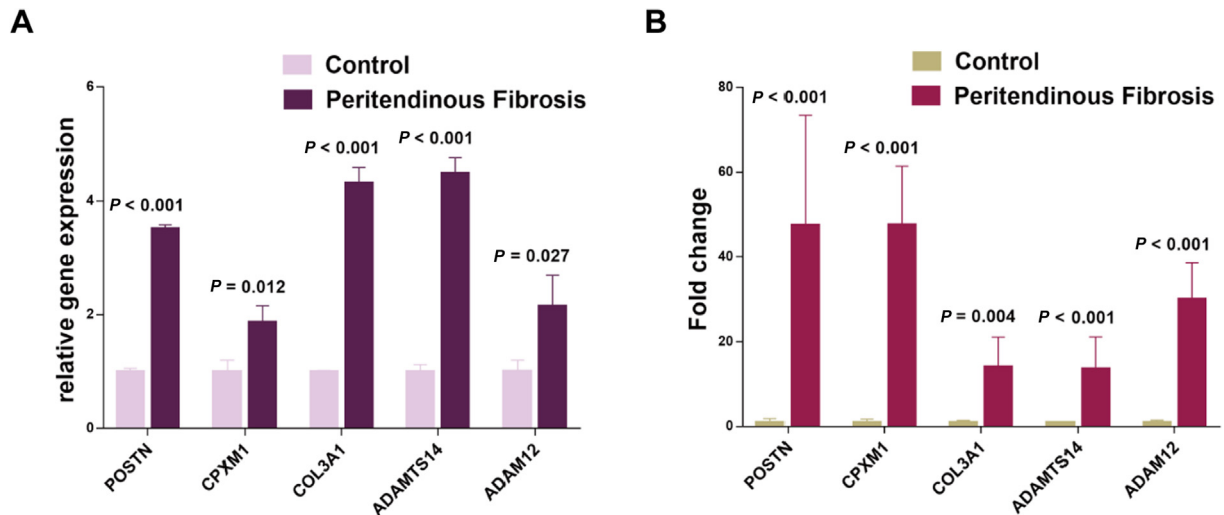
Fig. 5. qRT-PCR validation of differentially expressed mRNAs. (A) qRT-PCR verification of the expression profiles of 5 dysregulated mRNAs in fibrotic peritendinous tissues. (B) Fold changes of 5 dysregulated mRNAs in fibrotic peritendinous tissues identified by RNA-seq.

Fig. 6. GO analysis of differentially expressed genes. GO analysis of upregulated (A) and downregulated (B) mRNAs in fibrotic peritendinous tissues.

developmental processes, and positive regulation of biological processes (Fig. 6B). A KEGG analysis of differentially expressed mRNAs revealed that the upregulated mRNAs were associated with

35 pathways and that the downregulated mRNAs were associated with 66 pathways. Antigen processing and presentation, ECM-receptor interactions, the cell cycle, tumor necrosis factor signaling

pathway, and cytokine-cytokine receptor interaction were among the most enriched dysregulated pathways, suggesting that they are important for the progression of peritendinous fibrosis (Fig. 7A, B).

Co-expression of LncRNAs and mRNAs

Currently, the potential functions of lncRNAs can be inferred from lncRNA-mRNA co-expression networks. Eight differentially expressed lncRNAs were selected for inclusion in the co-expression network (PCC ≥ 0.990). The lncRNA-mRNA interaction network comprised 154 nodes, including eight lncRNAs (NR_038397, ENST00000518014, ENST00000414002, ENST00000429829, ENST00000602507, ENST00000602461,

ENST00000513626, and ENST00000602964) and 146 mRNAs (Fig. 8). These nodes formed 181 network pairs, including 116 positive and 65 negative correlations. The network shows that a single lncRNA may be correlated with several mRNAs and vice versa. Thus, interactions between lncRNAs and mRNAs likely mediate the development of peritendinous fibrosis.

Silencing of Dnm3os prevents profibrotic changes in primary tenocytes

Excessive cell proliferation and ECM deposition are two important features of peritendinous fibrosis. After TGF-β1 treatment for 24 h, the expression level of dnm3os was significantly increased (Fig. 9A). TGF-β1 also increased tenocyte viability (Fig. 9B). However, cell viability was significantly suppressed in tenocytes
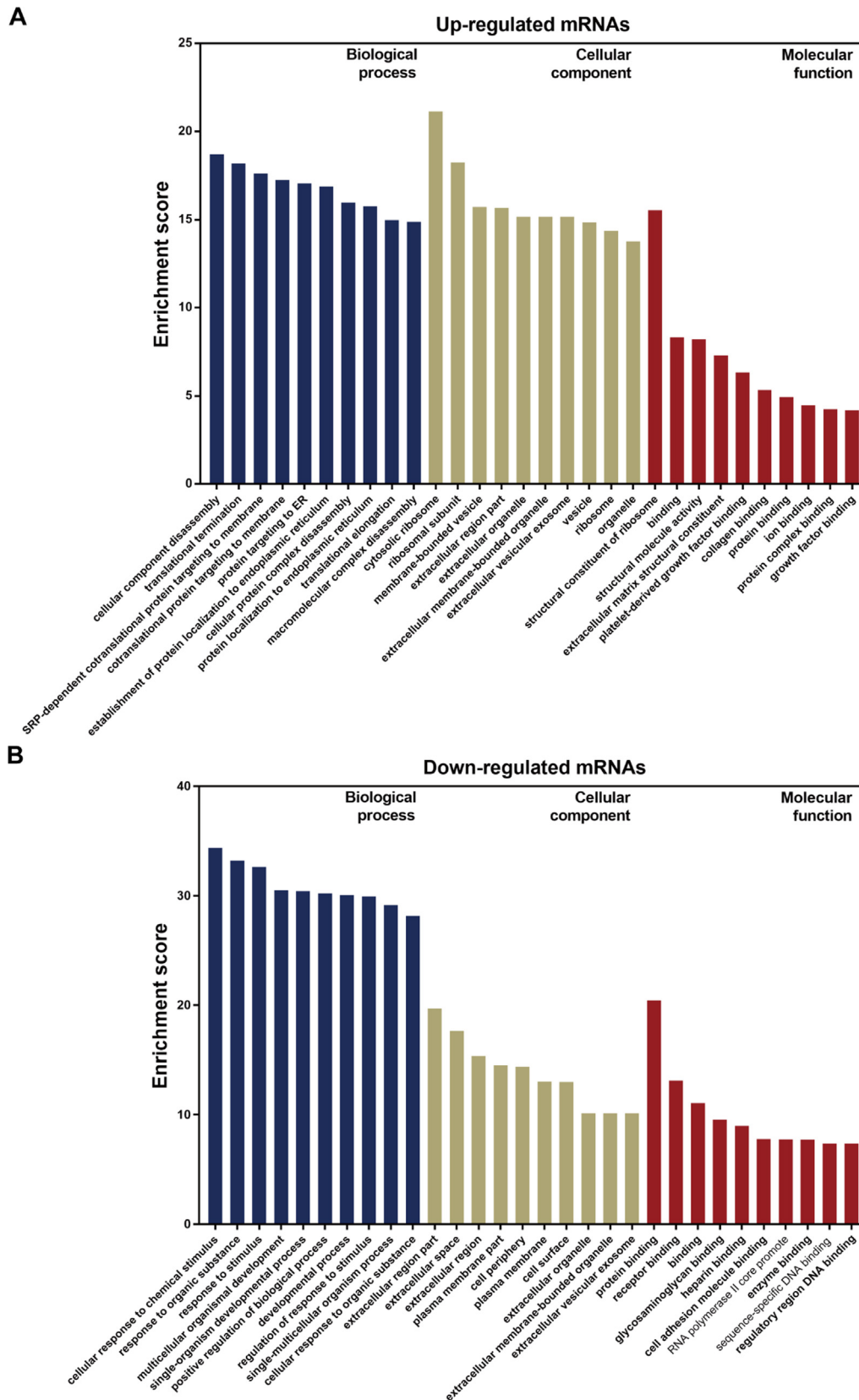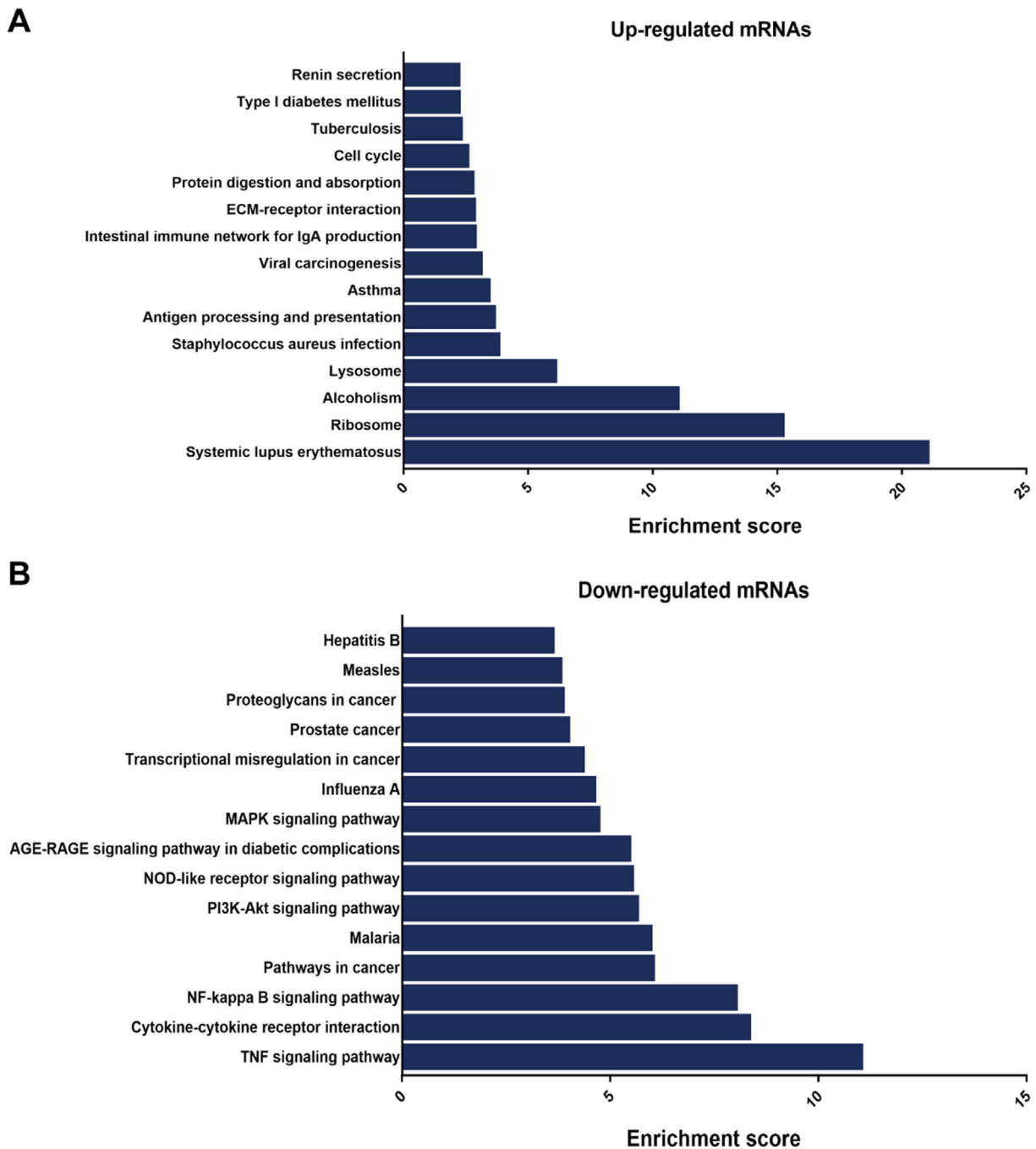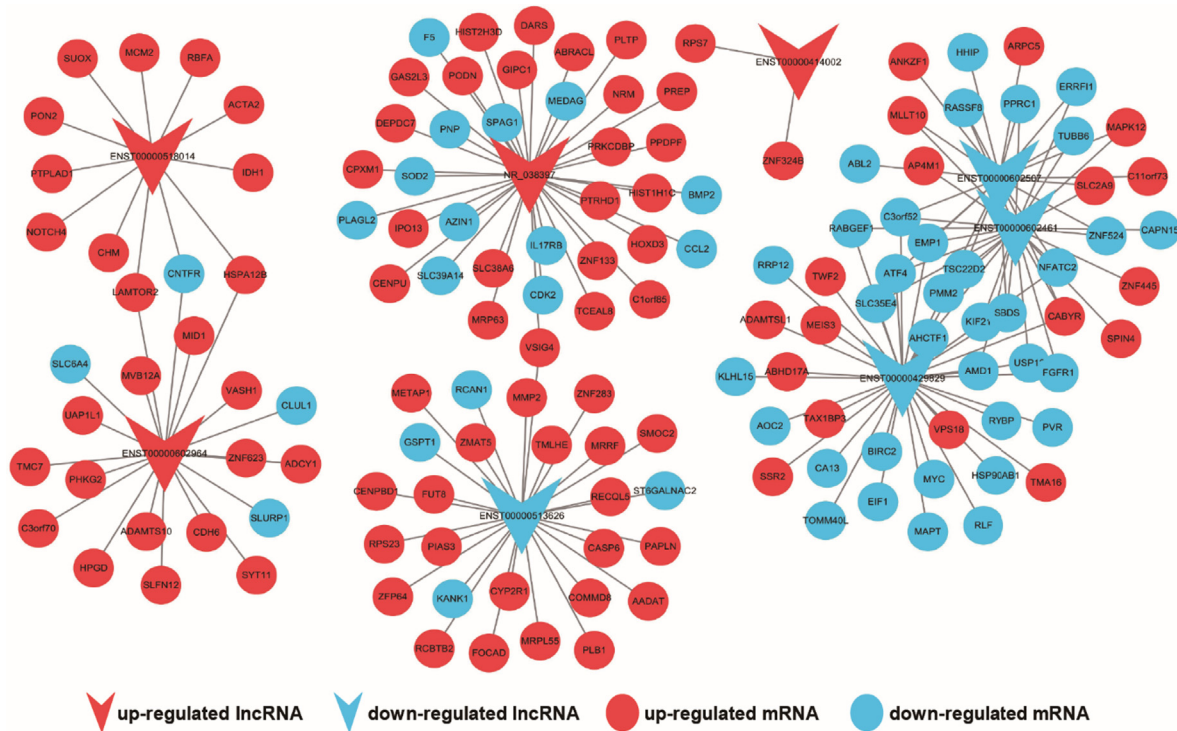

Fig. 7. KEGG pathway analysis of differentially expressed genes. KEGG pathway analysis of upregulated (A) and downregulated (B) mRNAs in fibrotic peritendinous tissues.

Fig. 8. LncRNA-mRNA co-expression network for eight dysregulated lncRNAs. The network was constructed based on Pearson correlation coefficients (absolute value of PCC ≥ 0.990). Upregulated mRNAs are shown as red circles, downregulated mRNAs are shown as blue circles, upregulated lncRNAs are shown as red triangles, and downregulated lncRNAs are shown as blue triangles.

transfected with dnm3os siRNA, compared with those transfected with scrambled siRNA. Moreover, TGF-β1 treatment also upregulated the expression levels of genes related to fibrogenesis, including col1, col3, α-SMA, and fibronectin 1. The expression levels of these fibrotic genes were decreased in tenocytes transfected with dnm3os siRNA, compared to those transfected with scrambled siRNA (Fig. 9C–F).

Discussion

Using RNA high-throughput sequencing techniques, recent studies have identified a number of lncRNAs that are differentially expressed in fibrotic diseases, providing a new direction for exploring the pathogenesis of fibrosis. However, the precise contribution of lncRNAs to peritendinous fibrosis is unknown. The lncRNA and mRNA expression profiles of normal and fibrotic peritendinous tissues were explored, for the first time, in this study to address this issue.

Using Illumina high-throughput sequencing, a total of 219 lncRNAs and 3403 mRNAs were identified that were differentially expressed between the two sample sets. These results were validated by qRT-PCR. Moreover, some of the dysregulated lncRNAs have been reported to be differentially expressed in other diseases [9,10]. COL1A1, COL3A1, and COL5A1, which are important components of the ECM, were upregulated, while other genes involved in fibrotic diseases, such as periostin (POSTN), a disintegrin and metalloprotease (ADAM)12, and ACTA2 were also dysregulated. ACTA2 is a marker of myofibroblasts, which are activated during fibrogenesis [11–13]. POSTN is a matricellular protein that binds to ECM components including collagen I and fibronectin and participates in collagen fibrillogenesis [14]. In a bleomycin-induced pulmonary injury model, fibrocyte-derived POSTN strongly stimulated TGFβ1 production and fibrocyte-myofibroblast differentiation [15]. The

ADAM12 level was found to be correlated with the initiation and progression of tissue fibrosis [16,17]. In ADAM12 transgenic mdx mice, skeletal muscle loss, fibrogenesis, and adipogenesis were significantly accelerated [18]. On the other hand, most of the differentially expressed lncRNAs and mRNAs in fibrotic peritendinous tissues are reported here for the first time.

The GO analysis showed that dysregulated genes were enriched in cellular component disassembly, translational termination, SRP-dependent cotranslational protein targeting the membrane, cotranslational protein targeting the membrane, and protein targeting the ER, suggesting that the tendon mounts an adaptive response to injury. Moreover, it was also noted that the molecular functions of dysregulated genes were associated with ECM structural constituents, collagen binding, and growth factor binding, i.e., the processes associated with ECM production and remodeling. The KEGG pathway analysis of dysregulated mRNAs revealed that dysregulated immune regulation, inflammation, ECM interactions, and the cell cycle are involved in fibrogenesis after tendon injury. Nuclear factor (NF)-κB is activated downstream of inflammatory cytokine receptors. Chen showed that NF-κB signaling was activated in fibrotic peritendinous tissues, whereas P65 inhibition prevented adhesion formation in rats [19]. Existing evidence has revealed that lncRNAs are also involved in NF-κB signaling regulation. A previous study showed that the lncRNA PACER sequestered the inhibitory subunit of NF-κB (p50), enhanced the formation of p65/p50 activating dimers, and promoted the synthesis of COX2 [20]. Another lncRNA, HOXD-AS1, has been reported to upregulate JAK/STAT target genes, including COX-1 and caspase-1 [21]. In recent years, aberrant arrest of the cell cycle has been shown to be critical in fibrogenesis; additionally, excessive cell proliferation and increased G2/M arrest have been observed in peritendinous fibrosis [22]. Furthermore, Li showed that Atg5 interference promoted G2/M phase arrest in proximal tubular epithelial cells and exacerbated subsequent renal fibrosis [23].
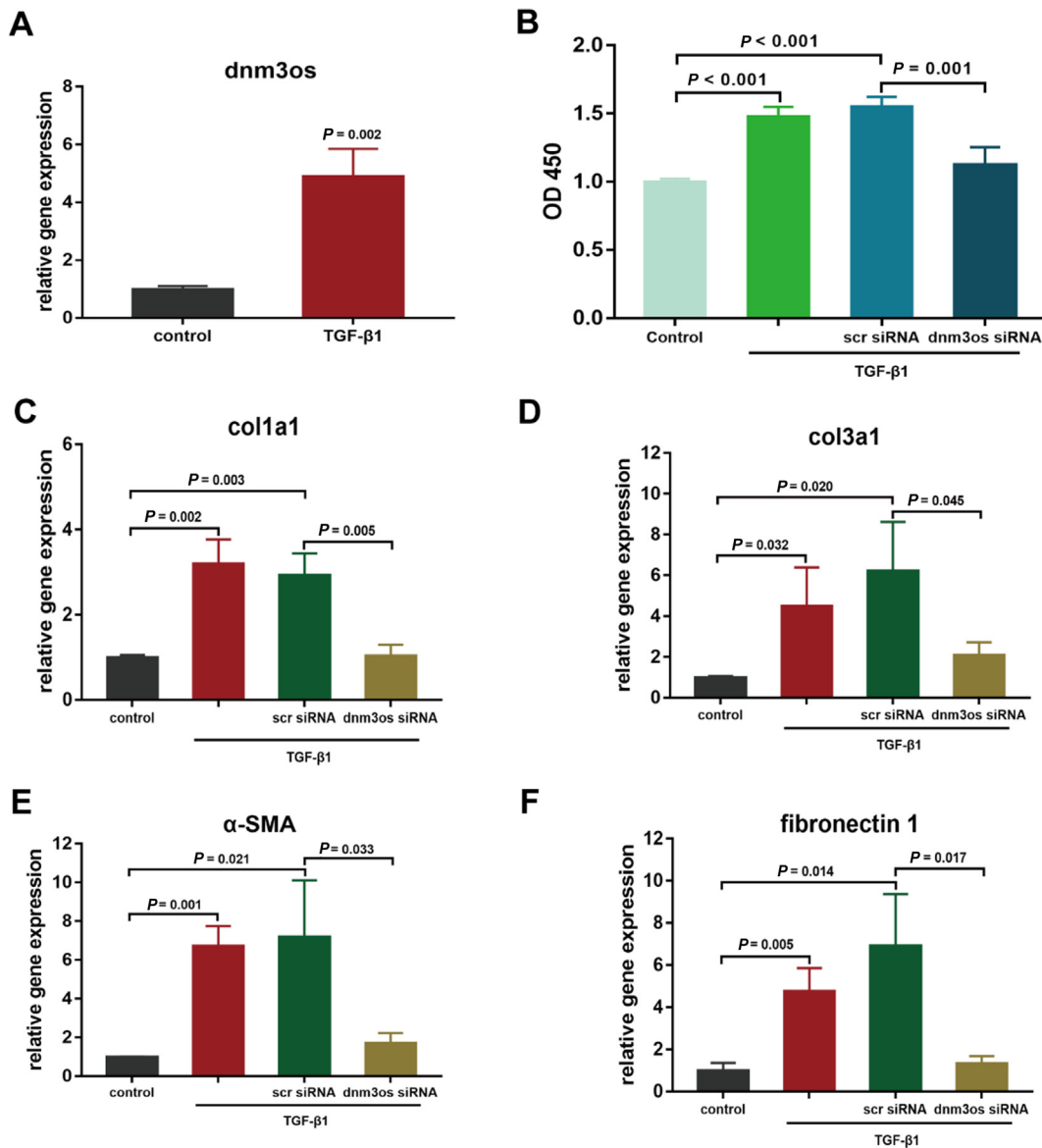
Fig. 9. Silencing of dnm3os prevents TGF-β1 induced fibrotic changes. (A) Dnm3os expression was increased in tenocytes treated with TGF-β1. (B) Cell viability after tenocytes were transfected with scrambled siRNA or dnm3os siRNA. Expression levels of col1a1 (C), col3a1 (D), α-SMA (E), and fibronectin 1 (F) after different treatments.

The major function of lncRNAs is the regulation of mRNA expression. However, the interactions between lncRNAs and mRNAs in peritendinous fibrosis have not been previously reported. To explore the potential role of lncRNAs in this process, a co-expression network between the selected lncRNAs and dysregulated mRNAs was further established. NR_038397, also known as DNM3 opposite strand/antisense RNA (DNM3OS), was among the most highly upregulated lncRNAs (6.5-fold change). NR_038397 has also been shown to be overexpressed in the cardiac tissue of heart failure patients. In contrast. Dnm3os-deficient mice showed restored peroxisome proliferator-activated receptor-δ signaling, improved cardiac contractility, and reduced interstitial fibrosis [9]. In recent years, epithelial-to-mesenchymal transition (EMT) has been proposed as an important mechanism in various fibrotic diseases [24,25]. Moreover, NR_038397 overexpression strongly enhanced EMT in ovarian cancer [26]. The co-expression network showed that NR_038397 expression was strongly correlated with that of prolyl endopeptidase (PREP) and protein kinase C, delta binding protein (PRKCDBP). PREP is a serine peptidase that can cleave short peptides (<30 amino acids) at the C-side of a proline residue. Existing evidence has shown that PREP mediates the formation of proline-glycine-proline, an important neutrophil chemoattractant, resulting in chronic neutrophilic inflammation in cystic fibrosis [27]. Previous studies have shown that the activation of extracellular signal-regulated kinase (ERK) signaling, a non-canonical form of TGF signaling, promotes fibrogenesis after tendon injury [21,28]. Meanwhile, the activation of PRKCDBP, localized in caveolae, activates ERK signaling and suppressed Akt signaling. [29]. In the present study, when dnm3os was silenced, cell viability and fibrotic gene expression were suppressed, suggesting that dnm3os plays a role in cell proliferation and ECM production. The co-expression network showed that the expression of minichromosome maintenance-2 (MCM2) was positively correlated with that of ENST00000518014. MCM2 is a highly conserved MCM that is involved in the initiation and elongation of DNA replication during the cell cycle. A previous study showed that the MCM2 expression level was positively associated with fibrosis progression in post-transplantation HCV hepatitis, suggesting that

MCM2 can predict early cirrhosis [30]. Moreover, the phosphorylation of the amino-terminal serines of *MCM2* facilitated chromatin loading and promoted cell-cycle re-entry from quiescence [31].

There were several limitations to this study. First, although RNA-seq revealed many differentially expressed lncRNAs between normal tendon and fibrotic peritendinous tissues, these lncRNAs require validation in a larger sample. Second although the functions of differentially expressed lncRNAs were predicted through co-expression analyses in this study, the precise mechanisms were not clarified. Additional studies are required to elucidate the various roles of lncRNAs in peritendinous fibrosis.

Conclusions

In conclusion, the results of the present study reveal a number of dysregulated lncRNAs that are potentially associated with the development and progression of fibrogenesis. These findings provide valuable insight into novel therapeutic strategies for the prevention and treatment of peritendinous fibrosis.

Acknowledgements

Conflict of interest statement

The authors have declared no conflict of interest.

References

[1] Manske P. Flexor tendon healing. J Hand Surg Br 1988;13:237–45.
[2] Juneja SC, Schwarz EM, O'Keefe RJ, Awad HA. Cellular and molecular factors in flexor tendon repair and adhesions: a histological and gene expression analysis. Connect Tissue Res 2012;54:218–26.
[3] Meng XM, Tang PM, Li J, Lan HY. TGF-β/Smad signaling in renal fibrosis. Fron Physiol 2015;6:82.
[4] Wynn TA, Ramalingam TR. Mechanisms of fibrosis: therapeutic translation for fibrotic disease. Nat Med 2012;18:1028–40.
[5] Novikova IV, Hennelly SP, Tung CS, Sanbonmatsu KY. Rise of the RNA machines: exploring the structure of long non-coding RNAs. J Mol Biol 2013;425:3731–46.
[6] Sun J, Zhang S, Shi B, Zheng D, Shi J. Transcriptome identified lncRNAs associated with renal fibrosis in UUO rat model. Front Physiol 2017;8:658.
[7] Li Z, Ouyang H, Zheng M, Cai B, Han P, Abdalla BA, et al. Integrated analysis of long non-coding RNAs (lncRNAs) and mRNA expression profiles reveals the potential role of lncRNAs in skeletal muscle development of the chicken. Front Physiol 2017;7:687.
[8] Wu C, Liu H, Zhang F, Shao W, Yang L, Ning Y, et al. Long noncoding RNA expression profile reveals lncRNAs signature associated with extracellular matrix degradation in kashin-beck disease. Sci Rep 2017;7:17553.
[9] el Azzouzi H, Leptidis S, Dirkx E, Hoeks J, van Bree B, Brand K, et al. The hypoxia-inducible microRNA cluster miR-199a∼214 targets myocardial PPARδ and impairs mitochondrial fatty acid oxidation. Cell Metab 2013;18:341–54.
[10] Damas ND, Marcatti M, Côme C, Christensen LL, Nielsen MM, Baumgartner R, et al. SNHG5 promotes colorectal cancer cell survival by counteracting STAU1-mediated mRNA destabilization. Nat Commun 2016;7:13875.
[11] Meng XM, Wang S, Huang XR, Yang C, Xiao J, Zhang Y, et al. Inflammatory macrophages can transdifferentiate into myofibroblasts during renal fibrosis. Cell Death Dis 2016;7:e2495.
[12] Darby IA, Zakuan N, Billet F, Desmoulière A. The myofibroblast, a key cell in normal and pathological tissue repair. Cell Mol Life Sci 2016;73:1145–57.
[13] Desmoulière A, Geinoz A, Gabbiani F, Gabbiani G. Transforming growth factor beta 1 induces alpha smooth muscle actin expression in granulation tissue myofibroblasts and in quiescent and growing cultured fibroblasts. J Cell Biol 1993;122:103–11.
[14] Kudo A. Periostin in fibrillogenesis for tissue regeneration: periostin actions inside and outside the cell. Cell Mol Life Sci 2011;68:3201–7.
[15] Ashley SL, Wilke CA, Kim KK, Moore BB. Periostin regulates fibrocyte function to promote myofibroblast differentiation and lung fibrosis. Mucosal Immunol 2017;10:341–51.
[16] Kerna I, Kisand K, Suutre S, Murde M, Tamm A, Kumm J, et al. The ADAM12 is upregulated in synovitis and postinflammatory fibrosis of the synovial membrane in patients with early radiographic osteoarthritis. Joint Bone Spine 2014;81:51–6.
[17] Taniguchi T, Asano Y, Akamata K, Aozasa N, Noda S, Takahashi T, et al. Serum levels of ADAM12-S: possible association with the initiation and progression of dermal fibrosis and interstitial lung disease in patients with systemic sclerosis. J Eur Acad Dermatol Venereol 2013;27:747–53.
[18] Jørgensen LH, Jensen CH, Wewer UM, Schrøder HD. Transgenic overexpression of ADAM12 suppresses muscle regeneration and aggravates dystrophy in aged mdx mice. Am J Pathol 2007;171:1599–607.
[19] Chen S, Jiang S, Zheng W, Tu B, Liu S, Ruan H, et al. RelA/p65 inhibition prevents tendon adhesion by modulating inflammation, cell proliferation, and apoptosis. Cell Death Dis 2017;8:e2710.
[20] Krawczyk M, Emerson BM. p50-associated COX-2 extragenic RNA (PACER) activates COX-2 gene expression by occluding repressive NF-κB complexes. Elife 2014;3:e01776.
[21] Yarmishyn AA, Batagov AO, Tan JZ, Sundaram GM, Sampath P, Kuznetsov VA, et al. HOXD-AS1 is a novel lncRNA encoded in HOXD cluster and a marker of neuroblastoma progression revealed via integrative analysis of noncoding transcriptome. BMC Genomics 2014;15(Suppl 9):S7.
[22] Zheng W, Song J, Zhang Y, Chen S, Ruan H, Fan C. Metformin prevents peritendinous fibrosis by inhibiting transforming growth factor-β signaling. Oncotarget 2017;8:101784–94.
[23] Li H, Peng X, Wang Y, Cao S, Xiong L, Fan J, et al. Atg5-mediated autophagy deficiency in proximal tubules promotes cell cycle G2/M arrest and renal fibrosis. Autophagy 2015;12:1472–86.
[24] Skrypek N, Goossens S, De Smedt E, Vandamme N, Berx G. Epithelial-to-mesenchymal transition: epigenetic reprogramming driving cellular plasticity. Trends Genet 2017;33:943–59.
[25] Shu DY, Lovicu FJ. Myofibroblast transdifferentiation: the dark force in ocular wound healing and fibrosis. Prog Retin Eye Res 2017;60:44–65.
[26] Mitra R, Chen X, Greenawalt EJ, Maulik U, Jiang W, Zhao Z, et al. Decoding critical long non-coding RNA in ovarian cancer epithelial-to-mesenchymal transition. Nat Commun 2017;8:1604.
[27] Gaggar A, Jackson PL, Noerager BD, O'Reilly PJ, McQuaid DB, Rowe SM, et al. A novel proteolytic cascade generates an extracellular matrix-derived chemoattractant in chronic neutrophilic inflammation. J Immunol 2008;180:5662–9.
[28] Jiang S, Zhao X, Chen S, Pan G, Song J, He N, et al. Down-regulating ERK1/2 and SMAD2/3 phosphorylation by physical barrier of celecoxib-loaded electrospun fibrous membranes prevents tendon adhesions. Biomaterials 2014;35:9920–9.
[29] Hernandez VJ, Weng J, Ly P, Pompey S, Dong H, Mishra L, et al. Cavin-3 dictates the balance between ERK and Akt signaling. Elife 2013;2:e00905.
[30] Marshall A, Rushbrook S, Morris LS, Scott IS, Vowler SL, Davies SE, et al. Hepatocyte expression of minichromosome maintenance protein-2 predicts fibrosis progression after transplantation for chronic hepatitis C virus: a pilot study. Liver Transpl 2005;11:427–33.
[31] Chuang LC, Teixeira LK, Wohlschlegel JA, Henze M, Yates JR, Méndez J, et al. Phosphorylation of Mcm2 by Cdc7 promotes pre-replication complex assembly during cell-cycle re-entry. Mol Cell 2009;35:206–16.